

# Knowledge-Guided Classification of Coastal Zone Color Images off the West Florida Shelf

Mingrui Zhang<sup>1</sup>, Lawrence O. Hall<sup>2</sup>, Frank E. Muller-Karger<sup>3</sup> and  
Dmitry B. Goldgof<sup>2</sup>

<sup>1</sup>Department of Computer Science  
Winona State University  
Winona, MN 55987-5838

<sup>2</sup>Department of Computer Science and Engineering

<sup>3</sup>Department of Marine Science  
University of South Florida  
Tampa, Fl. 33620  
hall@csee.usf.edu

**Abstract** A knowledge-guided approach to automatic classification of Coastal Zone Color images of the West Florida Shelf is described. The approach is used to identify red tides on the West Florida Shelf, as well as areas with high concentration of dissolved organic matter such as a river plume found seasonally along the West Florida coast over the middle of the shelf. The Coastal Zone Color images are initially segmented by the unsupervised Multistage Random Sampling Fuzzy-c Means algorithm. Then, a knowledge-guided system is applied to the centroid values of resultant clusters to label case I, case II waters, a dilute river plume (“green river”), and red tide. The domain knowledge base contains information on cluster distribution in feature space, as well as spatial information such as bathymetry data. Our knowledge base consists of a rule-guided system and an embedded neural network. From 60 images, after training the system, this procedure recognizes all 15 images which contained a river plume and 45 images without. The system can correctly classify 74% of the pixels that belong to the river plume, which provides a substantial advantage to users looking for offshore extensions of riverine influence. Red tides

are also successfully identified in a time series of images for which ground truth confirmed the presence of a harmful bloom.

## 1 Introduction

Satellite imagery in the visible range of the electromagnetic spectrum has proven to be of great value in quantifying the concentration of algae in marine environments. Since the early 1970's, many studies have focused on refining algorithms for estimating chlorophyll using ocean color imagery. Most previous studies estimated phytoplankton concentration using a simple ratio of two or three spectral bands, namely ratios of a blue or blue-green sensor channel (e.g. 443 or 520nm) to a green channel (e.g. 550nm) [1, 2, 3].

This simple band ratio may lead to serious errors in estimating biomass, if the algorithm is applied indiscriminately to all oceanic waters. Specifically, the algorithm fails in environments where the color of water is not a simple function of the amount of green pigment (chlorophyll) available within plants. Such optically complex situations are common in waters along continental margins (continental shelves, slopes, and coastal waters), where water color may be affected by large amounts of dissolved organic matter (DOM) and/or sediment discharged by rivers, bottom reflection, intense phytoplankton blooms, etc.

Remote sensing-derived information is imprecise in nature. The color of the ocean (or pigment concentration in the ocean) can change continuously or across sharp boundaries or fronts. The instantaneous-field-of-view (IFOV) of a sensor records the reflected radiance from heterogeneous mixtures of biophysical materials such as pigment, water, and suspended sediments. Multispectral satellite data contains much of this information, which could be lost by applying simplified empirical algorithms on massive amounts of data. Fuzzy set classification, which takes into account the heterogeneous and imprecise nature of the real world, may be used in conjunction with supervised classification algorithms to automatically separate various types of environmental conditions and go beyond the information gained by applying simplified algorithms. Wang [4] described a fuzzy supervised classification method which consists of two steps: the estimate of fuzzy parameters from the training data, and a fuzzy partition of spectral space. Wang's method has been applied to determine land-use classes in Landsat MSS images.

Automatic segmentation has been applied to multispectral medical images. Li et al. [5, 6], for example, proposed a knowledge-guided approach to automatic classification and tissue labeling of magnetic resonance (MR) images of the human brain. The MR brain image is initially segmented

by an unsupervised algorithm, then an expert system is used to locate a tissue or cluster and analyze it by matching it with a model or searching for expected features.

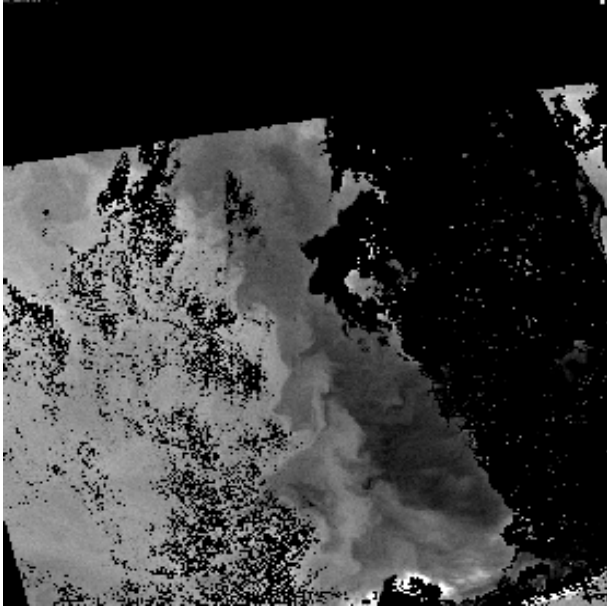
Remote sensing has been a strong application area for pattern recognition work. One important application is classification. The remotely sensed data have been classified using feed-forward neural networks [7, 8, 9], decision trees approaches [10], an expert system [11], or a rule-based system [12] by different researchers.

Though expert systems and neural networks have unique and sometimes complementary features, the integration of these techniques can be beneficial. Medsker and Bailey categorized the integration strategies into five models: stand-alone, transformations, loosely coupled, tightly coupled and fully integrated [13]. Approaches for transformations between expert systems and neural networks were discussed in [14]. Cohen and Hudson [15] incorporated techniques from approximate reasoning and a neural network. The neural network was used to determine, for example, the antecedent weighting factors and the threshold levels for rules.

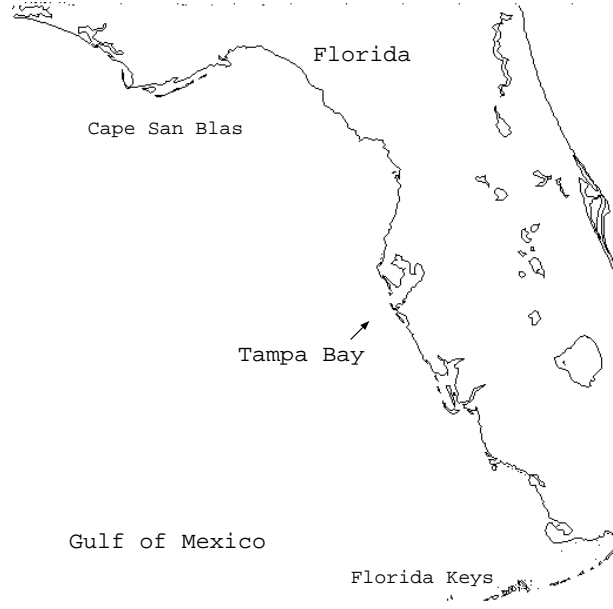
In the system we present in this paper, the knowledge based system is in charge of processing the images. A neural network is embedded in the knowledge base and used to label fuzzy clusters. The embedded system can be considered as a variation of a tightly-coupled integration of expert systems and neural networks. The rule-based component is also used to interpret the results of the neural network. This novel system is applied to ocean satellite images for automatic identification of different types of waters. When there are enough satellite images collected and ground-truthed for a specific region, the system can be trained and later used to process the unseen images.

Our initial work [16] developed the knowledge-guided system to recognize red tides from CZCS images using unsupervised Multistage Random Sampling Fuzzy-c Means (mrFCM) [17]. Here we describe an approach that uses this knowledge-guided system, which consists of rules and a neural network (NN), to identify phytoplankton blooms and a river plume from CZCS satellite images. Instead of using the fuzzy c-means clustering algorithm (FCM) [18], we use mrFCM, because the algorithm significantly reduces the computation time required to partition a data set into classes when compared with FCM.

Automatic identification and tracking of case I, case II waters and phytoplankton blooms from satellite images would provide an extremely useful tool to address resource management issues and scientific questions regarding the fate of organic material in the seas, and particularly along coastal environments. The Coastal Zone Color Scanner (CZCS) was a sensor operated by NASA between 1978 and 1986. It provided a large number of multispectral images for which domain-specific knowledge is available. The CZCS was a scanning radiometer aboard the Nimbus-7 satellite which viewed the ocean in six co-registered spectral bands 443, 520, 550, 670, 750nm,



(a) Band 443nm.



(b) West Florida Coast.

Figure 1: a) Coastal Zone Color Scanner (CZCS) Band 1 (443nm) image after atmospheric correction. b) the coast of Florida with areas of interest on the West Florida Shelf highlighted.

and a thermal IR band (10.5-12.5  $\mu\text{m}$ ). The first 3 bands were used to obtain estimates of the near-surface concentration of phytoplankton pigments, which modifies the spectral radiance backscattered out of the ocean. In this work, we use the 443, 520, 550, 670nm bands, and the pigment concentration fields derived from ratios of the 443, 520, and 550nm bands after atmospheric correction effected by the algorithms of Gordon et al. [1, 2]. Below we refer to the 443, 520, 550nm, pigment concentration and 670nm bands as CB1, CB2, CB3, CB4, and CB5 respectively.

Figure 1 shows the geographical area chosen for this study. Pixels on land and missing data are colored black in the figure; pixels of valid data are shown in different gray levels. We chose this area because it was covered extensively by the CZCS, and because substantial field information was available for the region. The “ground truth” of the historical CZCS image allows us to develop a sound system to identify specific phenomena.

Section 2 introduces background knowledge on red tides and the river plume observed in our region. Section 3 describes the approach used to search for images with specific bloom types or river plumes. The results are presented in Section 4 with a summary in Section 5.

## 2 Knowledge Base

Knowledge-guided systems can offer intelligent advice about or perform actions on segmented images. The knowledge-guided system attempts to apply human knowledge and mimic the human reasoning process, both of which are often fuzzy, or imprecise, in nature. Whenever knowledge about the area being studied is available, or if information about the relation of the expected classes after clustering in feature space is available, knowledge-guided clustering can be applied. Our knowledge base is used to guide the clustering process. Two primary sources of knowledge used in our approach are: 1) domain knowledge; 2) cluster distribution in feature space.

### 2.1 Domain Knowledge

Domain knowledge refers to the various types of waters expected in an image and which should be identified as different types of clusters in a specific region. In this section, we introduce background knowledge about red tides, river plumes, case I and case II waters, and then examine algorithms and heuristics used by oceanographers to separate these as different domains.

The most severe red tides along the West Florida coast are brought about by a population explosion of a specific dinoflagellate[19], namely *Gymnodinium breve*. The blooms typically seen begin in the Gulf of Mexico 40-80 miles offshore and move toward the coast[20] (Figure 1(b)). These monospecific blooms can kill marine animals not only because of a potent neurotoxin within the blooms, but also by depleting dissolved oxygen in the water. Blooms represent population densities of more than  $5 * 10^4$  organisms/liter. A mathematical model that simulates the spectral curves of the remote-sensing reflectance of blooms of red tides was developed by Carder and Steward [21]. Their model simulates the effects of backscattering from water, phytoplankton, and detritus, etc.

Another phenomena that is observed routinely over the West Florida Shelf is a river plume, which is clearly detectable in CZCS images. The plume has high concentration in the CZCS pigment band, and it occurs mainly during spring. High pigment concentrations persist 1-6 weeks in a pattern which extends more than 250km southward along the shelf from Cape San Blas (Figure 1(b)). Gilbes et al. [22] suggested the plume is associated with seasonal discharge from rivers along the northwest Florida coast. Trapped in a southward circulation, the plume is established by seasonal steric height differences (density-driven) between the shelf and deep Gulf of Mexico waters. During dinoflagellate blooms, biomass in surface waters varies from  $2 - 30mg/m^3$  Chl-a. Otherwise, concentrations range  $0.1 - 2mg/m^3$  Chl-a in the Gulf of Mexico, with higher concentrations over the shelf areas [23]. The river plume over the West Florida Shelf

has been referred to as the “green river”. The terms river plume and “green river” are used interchangeably in this paper.

Morel and Prieur [24] have optically classified seawater according to its constituents. Those waters for which phytoplankton and their covarying detrital material play the dominant role in determining the optical properties are called case I waters. Those waters for which inorganic suspended material (such as might be resuspended from the bottom in shallow areas) plays an important role or in which either detrital, DOM, or both, are uncorrelated with Chl-a, are referred to as case II waters. Most of the open ocean waters are case I. According to the bio-optical algorithm widely used for CZCS [2], some case I waters (e.g. open ocean) may have pigment values (CB4) of 0.025-5.4mg/m<sup>3</sup>. There have been some attempts to determine case II waters automatically from CZCS data, but most of these focus on coccolithophore blooms on case II water. Attempts to examine other types of case II waters, specifically those with high concentration of colored DOM, has been limited by the radiometric characteristics of the CZCS [25].

One approach that can help identify case II waters involves prior knowledge of the depth of coastal waters. Waters shallower than 25m may be automatically classified as case II waters [26]. This approach is now used for generating SeaWiFS products by NASA[27]. The advantage of this approach is its simplicity, but it is not accurate. Though the bio-optical algorithms of [2] can be used to define case I water, they do not provide information for classification of case II waters. This paper attempts to develop an imaging-based system to classify case I and case II waters using mrFCM under the control of a knowledge-guided system.

## 2.2 Cluster Distribution in Feature Space

Seawater is basically classified into case I and case II waters according to its optical properties. Both red tides and the “green river” occur on case I **and** case II waters. In this study, because of our special interest in red tides and the “green river”, we consider them as separate classes even though they can be geographically overlapping. Hence, we search for 4 classes in this study, namely case I water, case II water, red tides, and the “green river”.

Twenty five images were given to oceanographers at the University of South Florida for identification of different types of phytoplankton blooms (or ground truthing.) These oceanographers have first-hand knowledge of the various blooms in the region. **Eighteen** ground-truthed images were chosen as training images, from which we generated heuristic rules and trained a NN. Our knowledge-guided clustering approach is based on over-clustering the satellite image, and labeling

regions of interest produced by the over-segmentation. Our over-clustering approach is designed to provide maximally homogeneous clusters and works as follows. The number of objects in CZCS images is 4 (red tide, “green river”, case I and case II waters), we deliberately partition the data set into 12 classes empirically. This approach is designed to reduce the chance and frequency that pixels from different classes are combined into one class at the cost of splitting some true classes into multiple clusters. This step is necessary because case I, case II waters, “green river” and red tides are classes that frequently overlap or intersect in their bio-optical properties and in their feature space.

Heuristic rules based upon different 2-D projections of cluster centers which identify red tide clusters have been developed from the training images. The single training image for red tide was selected because there is conclusive evidence that a large scale bloom observed off the West Florida Shelf in November 1978 was a red tide. The rules enable the classification of some clusters. All pixels belonging to a cluster with a membership value greater than a predefined threshold will be removed from further processing. The training images are also used to train a NN for the identification of case I and case II waters, and further, to identify river plume. The NN was not used for recognition of red tides because there were too few red tide training images. Instead, we inspected 2-D projections of cluster centers and manually extracted rules. The NN was trained with the centroid values of clusters of the training images. The specific rules and the training of the NN are discussed in the next section.

### 3 Classification of CZCS Images

A satellite-data processing software package developed at the University of Miami, DSP [28], was used to generate the CZCS image features, calculate the water-leaving radiance of the 3 visible bands and a near infrared band, and pigment concentration. Each processed CZCS image consisted of 5 useful bands. Each band is treated as an intensity image. These images were mapped to  $512 \times 512$  pixel, 8 bit resolution. Therefore, each pixel to be clustered has 5 features associated respectively with bands 443, 520, 550, and 670nm, and the pigment concentration.

Our knowledge-guided system operates as shown in Figure 2. The multiple bands of CZCS images are provided along with ancillary data (bathymetry) to the system. Scientists have systematic knowledge about the geography or phenomena of the area studied. Indeed, attempts to improve the accuracy and the quality of remote-sensing-derived classification by incorporating ancillary data in the classification process have been quite successful [29]. Ancillary data consists of spatial or non-spatial information that may be of value in the image classification process. In

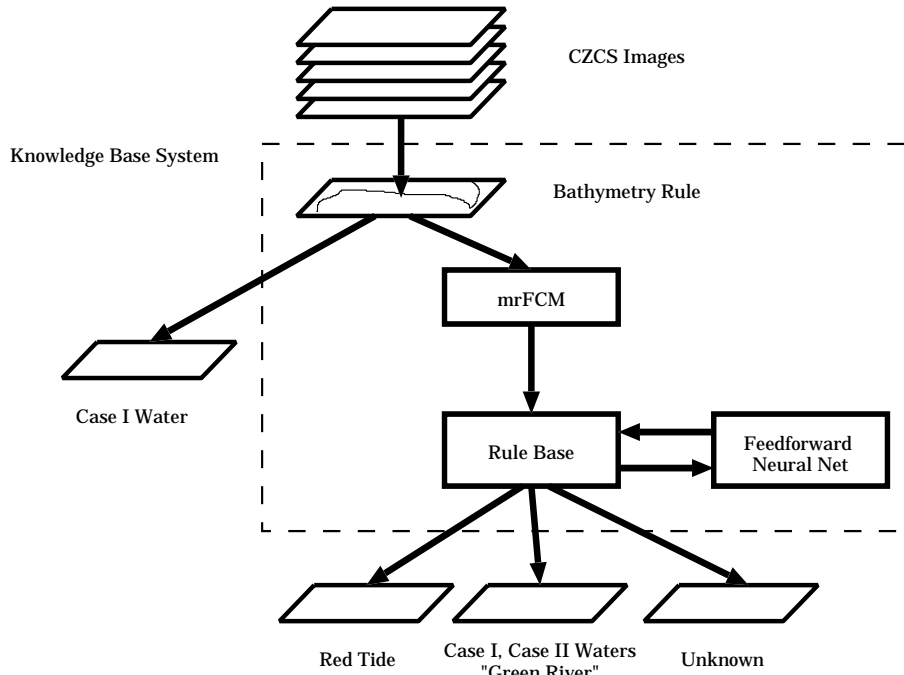


Figure 2: Integrated rule-based and neural network system.

this work, water depth is used prior to clustering to subdivide the images into two regions, case I water and the mixture of case I and case II waters. For this study focusing on the West Florida Shelf, pixels with water depth deeper than 300m were considered to be oceanic case I waters based on the definition of a shelf break at 250m, and were not of interest to this study. Hence they were excluded from clustering. The goal was to reduce computation effort in processing these CZCS images by using our domain knowledge. Remaining pixels were segmented by the mrFCM clustering algorithm. Subsequently, rules were used to determine the presence of red tides, given any red tides exist. A trained NN is embedded in the knowledge-guided system to differentiate between case I and case II waters, and identify “green river” after mrFCM segmentation.

The feedforward, backpropagation neural network [30] derives its computing power through its massively parallel distributed structure and its ability to learn and therefore generalize. A neural network consists of neurons, modeled as nonlinear devices. Nonlinearity is needed here because the distribution boundary of cluster centers of different water types is nonlinear. The clustered multi-band satellite images provide multi-band cluster features. Extraction of heuristic rules from the multi-dimensional feature space is not a simple task for humans. The NN provides a tool for automated extraction of knowledge from the distribution of cluster centers. In this work, a rule-based expert system tool, CLIPS [31], is used to organize the whole system.

```

IF( The depth is deeper than 300m )
THEN( It is case I water )

```

Figure 3: Rule to separate pixels with depth deeper than 300m.

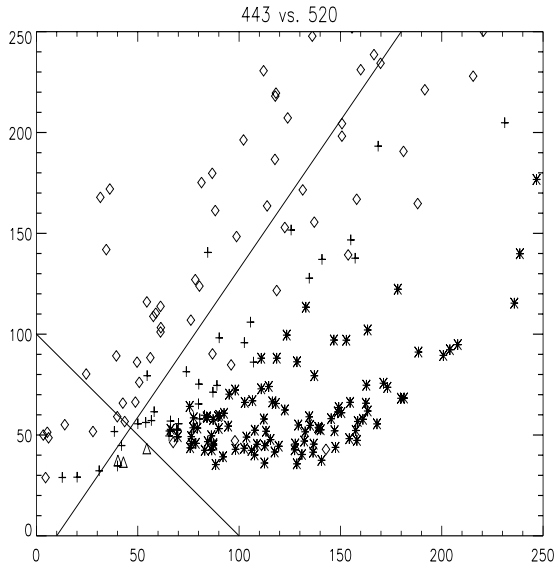
### 3.1 Heuristic Rules for Recognition of Case I Water and Red Tide

The rule shown in Figure 3 is first applied to identify some case I waters using bathymetry information. The identified waters are removed from further processing. Next, the mrFCM algorithm is used to segment the remaining pixels in CZCS images. During training, the cluster centers obtained from mrFCM are used to acquire the knowledge of pattern distribution in feature space. Based on the 4 pattern classes of interest (red tides, “green river”, case I, and case II waters), each CZCS image (with 5 bands) is clustered into 12 classes. Each class has a cluster center  $\langle \text{CB1, CB2, CB3, CB4, CB5} \rangle$ , corresponding to bands 443, 520, 550nm, the pigment concentration and 670nm respectively. Figure 4(a) shows the 216 cluster centers of the 18 training images projected onto the CB1-CB2 space, corresponding to the 443 and 520nm bands in the initial segmentation.

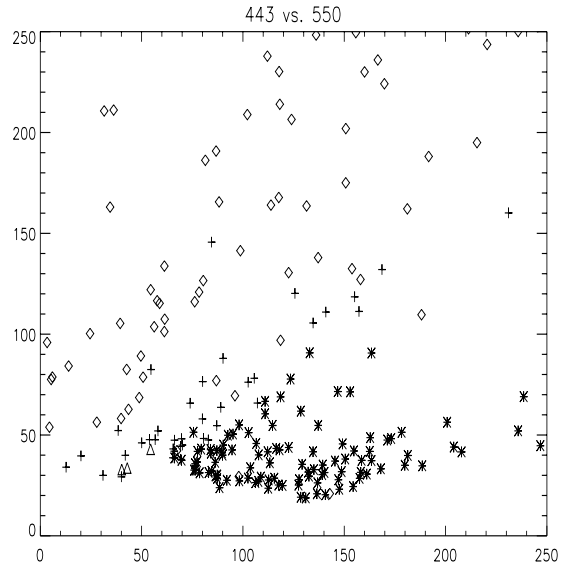
The knowledge of the class center distribution can be used in locating regions of interest for focus-of-attention and the separation of different types of waters. Figure 4(a) shows that red tide clusters (triangles) appear in the lower left part of Bands 443-520 feature space between the separation lines. Figure 5 shows the rule which is visually extracted from Figure 4 to identify red tide clusters. The rules and the NN use its centroid values to identify the cluster. The rule in Figure 5 provides a threshold function that allows us to quickly remove pixels representing red tides. The pixels which belong to clusters with centroid values satisfying the rule have very strong red tide water membership and thus are identified and removed from further consideration. We take an  $\alpha$ -cut of 1 (all pixels with membership in the cluster greater than or equal to  $\alpha$  are red tides.) Clearly, pixels with membership in the range  $[0.7,1)$  might be included as red tides. However, without pixel-level ground truth we choose a conservative classification approach.

### 3.2 Training the Neural Network

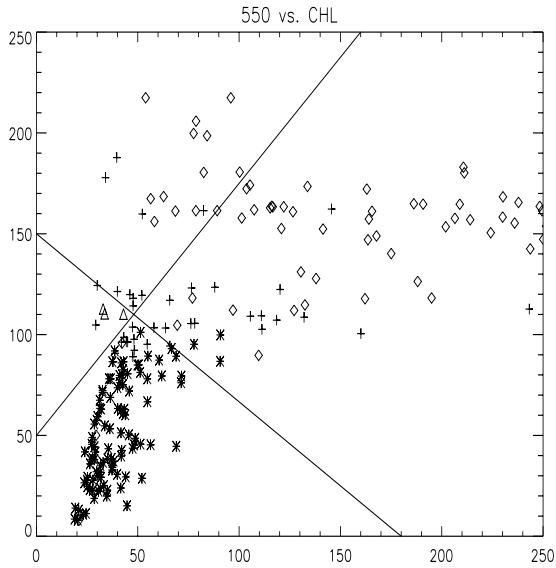
After the removal of red tides and some case I water by our rule set, we are left with pixels which represent case I, case II waters, and “green river”. The NN has been trained using the quick-propagation algorithm [32] to recognize the remaining types of waters after clustering. The quick-propagation algorithm is a variation on the backpropagation learning algorithm that



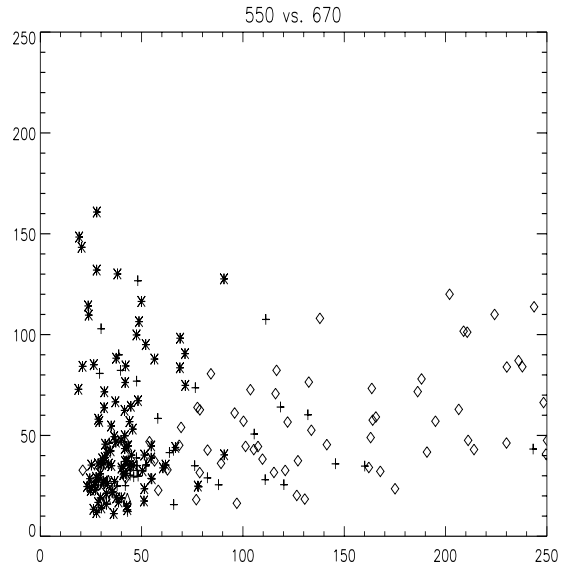
(a) Bands 443, 520



(b) Bands 443, 550



(c) Bands 550, Pigment



(d) Bands 550, 670

Figure 4: Class centers in feature space after clustering. Case I, case II waters are indicated by star and diamond. Red tides and river plumes are indicated by triangle and plus. The lines in (a, c) correspond to the thresholds to identify the red tides.

```

IF( CB2 < 100 - CB1 )
AND
( CB2 < 1.47*CB1 - 14.7 )
AND
( CB4 < 150 - 0.83*CB3 )
AND
( CB4 > 1.25*CB3 + 50 )
THEN( It is Red Tide )

```

Figure 5: Rule to recognize red tides.

uses a second-order weight-update function, based on measurement of the error gradient at two successive points, to speed up convergence. The number of input neurons in our network are 5 (Figure 6), they are the centroid values of a cluster. We use 3 outputs to represent the 3 types of water we are seeking to identify.

Since the system is developed for the classification of multispectral satellite images and the remote sensing images have a number of spectral bands, the use of a neural network to identify cluster centers becomes necessary. For example, the image collected by the Airborne Visible/Infrared Imaging Spectrometer(AVIRIS) has 224 spectral bands. Visually identifying heuristics in such a high dimensional space by human beings becomes inefficient or impossible. The neural network approach provides a general means to label fuzzy cluster centers. Though algorithms other than neural networks (e.g. decision trees[33] or the k-nearest neighbor) can be used for this purpose, to be consistent with our previous work, we choose to use a neural network in this system.

The ultimate objective of a pattern classifier is to achieve an acceptable rate of correct classification; this criterion is used to judge the effectiveness of a particular neural network architecture. Reflecting practical approaches to the problem of determining the optimal number of hidden layers and neurons, the criterion used is the smallest number of hidden layers and neurons that yield the best performance. The performance measure of the NN is based on cluster identification, namely the percentage of clusters that can be correctly identified by the NN on training images.

In this training experiment, 18 images were selected as a training set. The training set is further partitioned into two subsets: 1) seventeen images used for training the network, 2) one image used for evaluation of the performance of the network. For each network structure, the partition is repeated 18 times with different image assigned as the evaluation image each time (i.e. leave-1-out testing.) The best-performing network is then trained on the full training set. Table 4 shows that 16 hidden units yields the best performance (90% on a 10-fold cross validation

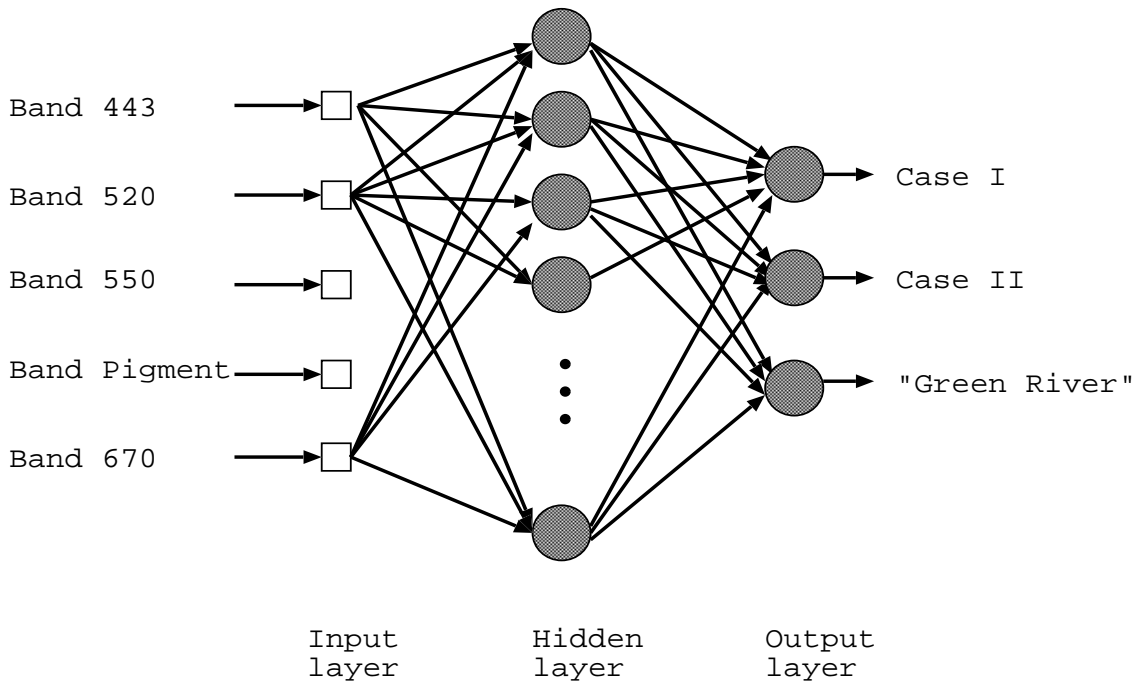


Figure 6: Neural network with one hidden layer, 10-20 neurons.

Table 1: Performance Measures of Neural Networks Under Different Network Configuration.

	One Layer				
Neurons	10	15	16	17	20
Correct (%)	71	80	90	74	65
SSE	0.41	0.40	0.36	0.36	0.38

experiment with labeled data.) The experimental study began with 1 hidden layer with 10 neurons as the starting point. The number of epochs was chosen so that the Sum Squared Error (SSE) is eventually stable. Note that small SSE does not necessarily imply good generalization[34].

We use a 1 hidden layer NN with 16 neurons. Although the average SSE for two-hidden-layer neurons is lower than that of one-hidden-layer neurons in our experiments, the average rate of correct classification does not show improvement and we utilize the simpler architecture. The architecture of the NN is shown in Figure 6.

Table 2: Summary of Red Tides (RT) and “Green River” (GR) Images.

	Ground Truth		
	RT (pixels)	GR (pixels)	None
Training	1 (4030)	10 (189800)	7
Testing		5 (83210)	2
Total	1 (4030)	15 (273010)	9

```

IF( Output of NN is within 10% of another output )
THEN( It is Unknown type of water )
ELSE( It is the class of NN output )

```

```

IF( Image was taken in the fall )
THEN( There is NO green river )

```

```

IF( Pixels are on the east coast of Florida )
THEN( It is NOT green river )

```

Figure 7: Rules applied to the network outputs.

### 3.3 Rules After the Neural Network

The NN is integrated into our knowledge-guided system, with rules (Figure 7) applied to the outputs of the network. The outputs from the NN range from 0 to 1, if there is any output within 10% of another output, the cluster should be considered of unknown type. Otherwise, the maximum network output is chosen as the network result (the first rule in Figure 7). For a complex task, a NN alone sometimes is not able to fully accomplish the task (e.g. geographic information on the “green river” is not easily utilized by the network). According to our domain knowledge about the “green river”, this phenomena occurs periodically over the West Florida Shelf in the Spring. Hence, the second and the third rules in Figure 7 take temporal and geographic information into account.

## 4 Results

In addition to the 25 ground truth CZCS images (Table 2), we processed 35 additional images using the DSP software package. The images span the time period from 1978 to 1986. Besides

focusing on the time periods when the red tides or river plume are expected to happen, we intentionally chose images covering different seasons each year to reflect the seasonal variations of the ocean currents and river runoff. Of the twenty-five images given to oceanographers for identification of different types of water, one image from 14 November 1978 has been positively recognized by oceanographers as containing red tides [35, 20]. Fifteen of the images are recognized to contain river plume. The training set consists of 18 images, one image with red tides, 10 images with river plume and 7 images with neither. The other 7 ground-truthed images are used as a testing set for our system. Table 2 shows the distribution of images.

After running 18 training images through the system, each clustered region on the CZCS image was inspected together with its five intensity feature cluster centers. The heuristic rules previously discussed were then extracted and implemented in our system. The NN is trained on the centroid values of clusters of the training images. We then apply the system to both training and testing images. The confusion matrix is computed and summarized in Table 3. Due to the fact that we have just one ground-truthed image for red tide, the pixel-level training and evaluation are done on this image.

Table 3: Confusion Matrix (by percentage) for Recognition of Different Types of Waters Using Knowledge-Guided System.

Classified as:	Red Tide	Green River	Case I	Case II
Red Tide	82	0	7	11
Green River	0	74	9	17
Case I	0	5	81	14
Case II	3	16	5	76

Our system can successfully recognize all 15 images with river plume and correctly identify another 10 images without river plume among 25 ground truth images. No river plume was found by our system on 35 non-ground-truthed images. Both results were presented to and confirmed by oceanographers at the University of South Florida, Marine Science Department. Due to the fact that we have one ground-truthed image for red tide, the training and evaluation are done on one image with the result serving as an upper limit on performance. Table 3 shows the percentage of pixel-level correct classification for the river plume which is 74%. Two difficulties contribute to this rate. First, it is difficult for an oceanographer to recognize the river plume in the case II water based on historical CZCS images (i.e. ground truth is approximate). Second, separation of river plume from other types of phytoplankton blooms (e.g. upwelling plume along the west coast of

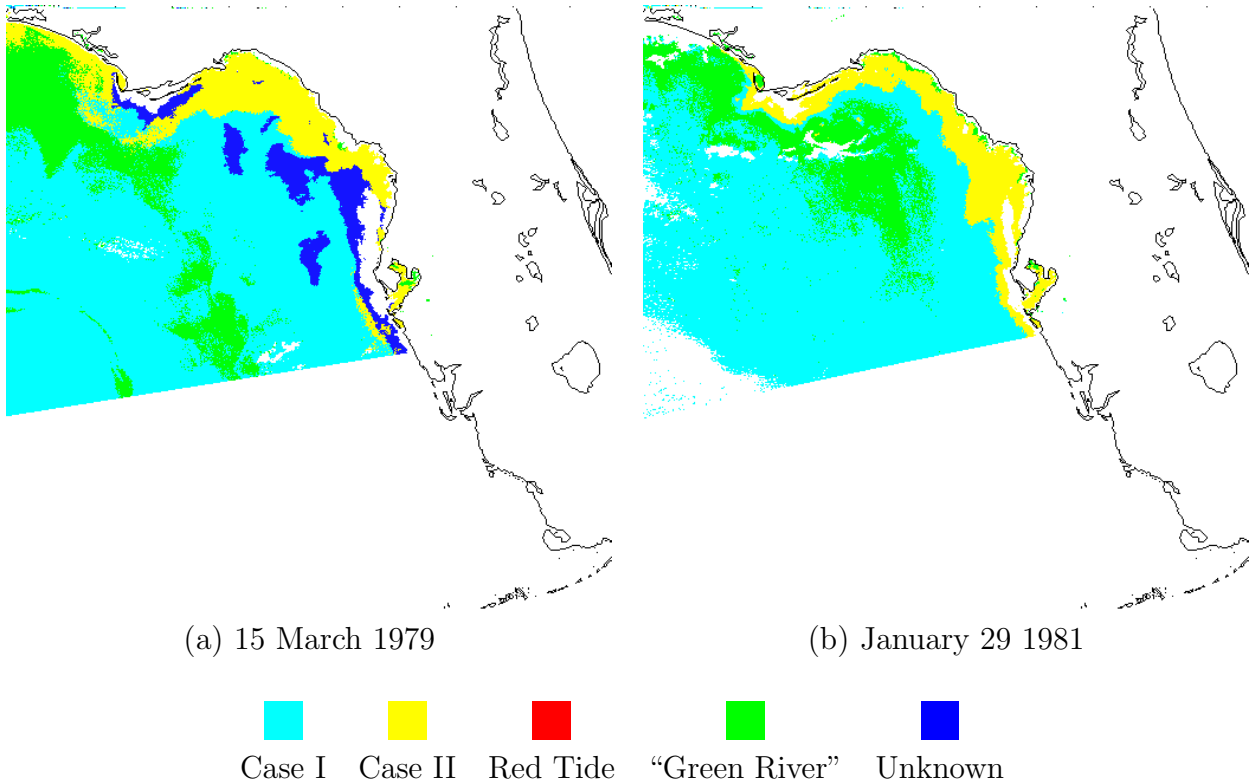


Figure 8: CZCS images with river plume after processing by the knowledge-guided system.

Florida) is difficult, due to similar optical properties between riverine plume and upwelling plume in the CZCS images. Besides these difficulties, the result is in large part due to the few bands available on the CZCS, and the limited radiometric quality of the sensor.

The CZCS time series allowed us to track the spatial extension of the river plume phenomenon in the area of the West Florida Shelf, for example, on March 1979 and January 1981 images (Figure 8). The plumes were detected by our system in all CZCS images where they occurred between 1980 and 1986 during the spring. These automatically identified plumes are consistent with the study by Gilbes et al.[22], though their study focused on understanding the formation of the plume.

#### 4.1 Comparison With Other Approaches

As a comparison to the knowledge-guided system, a neural network is trained with the “quick-prop” algorithm [32] to identify each pixel of the image. The *10-fold cross-validation* approach was repeated for neural networks to choose the architecture. Several network training runs were conducted using different numbers of hidden units. Eventually, a network with one hidden layer

of 28 neurons was chosen as the optimum architecture for the problem. To form a training set for the NN algorithm, 2000 pixels were randomly selected from the training images for each water type. The training set was 8000 examples. The rest of the red tide pixels and all image pixels from the testing image set form the testing set. After training the stand-alone NN, the trained NN was applied to the testing set. Table 4 shows the results. The results in Table 4 are significantly less accurate than those obtained with the knowledge-based system. There are significant number of green river pixels misclassified into red tide, and vice versa.

Table 4: Confusion Matrix (by percentage) for Recognition of Different Types of Waters Using Neural Network.

Classified as:	Red Tide	Green River	Case I	Case II
Red Tide	20	15	0	65
Green River	17	60	1	22
Case I	0	5	85	10
Case II	23	6	1	70

The k-nearest neighbor(kNN) algorithm was also applied to the same training and testing sets. The Euclidean distance between an unlabeled pixel and each labeled pixel is calculated. The distances are ranked and the  $k$  minima ( $k=7$ ) are selected. We count the frequency of each class labeled for the selected minima and the majority is chosen as the label for the pixel. The results from application of the kNN to the testing set are listed in Table 5. The results with kNN are better in recognizing Case II water than those with the NN, but worse in green river recognition. It is worse than the knowledge-based systems at recognizing both types of waters as well as red tide. To reduce the false positives in identifying images with the NN and kNN, a decision threshold at an image level can be implemented [36].

Table 5: Confusion Matrix (by percentage) for Recognition of Different Types of Waters Using k-nearest Neighbor Algorithm.

Classified as:	Red Tide	Green River	Case I	Case II
Red Tide	24	32	1	43
Green River	20	50	2	28
Case I	2	4	76	18
Case II	10	3	2	85

Compared to the Table 3, the knowledge-guided system outperforms the neural network and kNN approaches in identifying the "green river". As the "green river" occurred on both case I and case II waters, it was misidentified as case I or case II waters by the neural network or the kNN algorithm. This misclassification can not happen in the knowledge-guided system, as the "green river" and the red tide normally happen in the different time period and we can easily implement heuristic rules using time information to distinguish them.

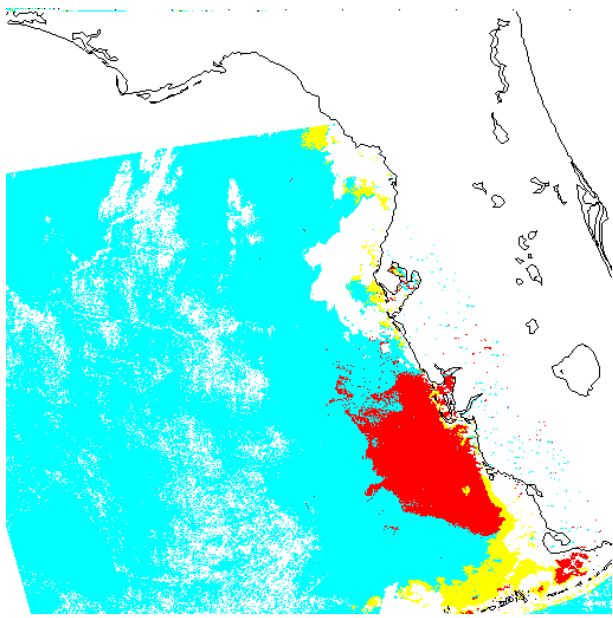
## 4.2 Red Tide

To show the ability to monitor red tides and classify case I and case II waters, we processed an additional 35 images. Red tides were found by the system on only 4 images which span the time period from 14 November to 2 December 1978. It was not found in any of the other 56 images, although none of these are known to contain red tides (they can not be proven to be devoid of red tide blooms either). There is reason to believe that 40 images do not contain red tides as they are from the wrong time of year for red tide blooms. Results shown in Figure 9 indicate that the red tide in 1978 lasted 4 weeks, starting from 14 November 1978. Note that case II water lies near the coast, as expected, and that red tides are recognized in both Case I and Case II waters. Figure 10 shows the classification of Case I and Case II waters from an image found to be without red tides and/or river plume.

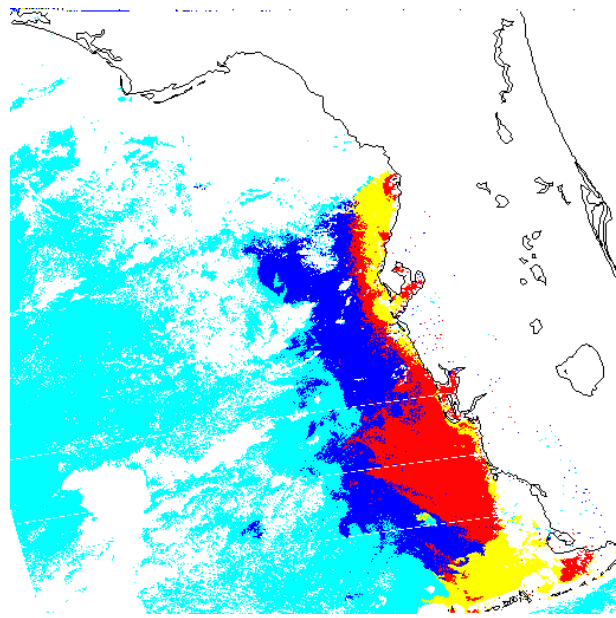
## 5 Conclusions and Future Work

Satellite imagery in the visible range of the electromagnetic spectrum has proven to be of great value in quantifying the concentration of algae in marine environments. Most algorithms used in remote sensing of chlorophyll-a plus the associated phaeophytin-a are of the spectral ratio type, which are considered valid only for Case I water. Our approach provides a knowledge-guided system to automatically separate case I from case II water and to track phytoplankton blooms like red tides and river plume phenomena on both types of water. By training the system on a set of satellite images containing the pattern classes, we provide a new technique for marine and environmental scientists to track the various types of blooms in the ocean.

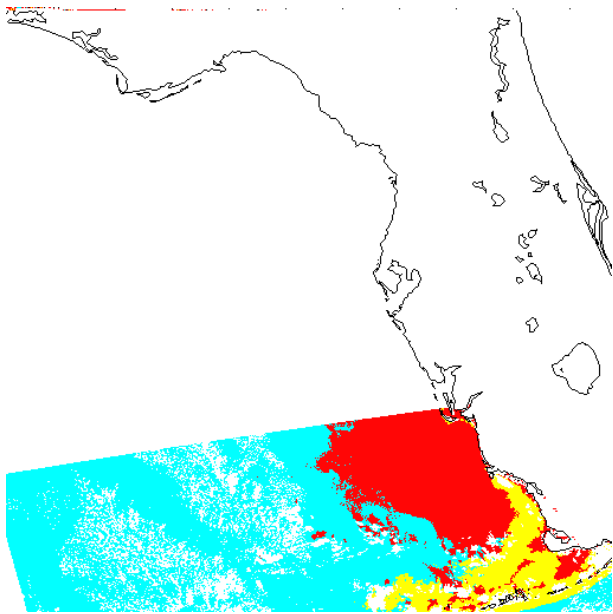
Our results show that the system can successfully recognize all images with the West Florida Shelf river plume and correctly classify images without river plume among 25 ground truth images. In those images with a plume, the system correctly classified 74% of the river plume pixels. The system also successfully identifies the known red tide that occurred in 1978. On the pixel-level,



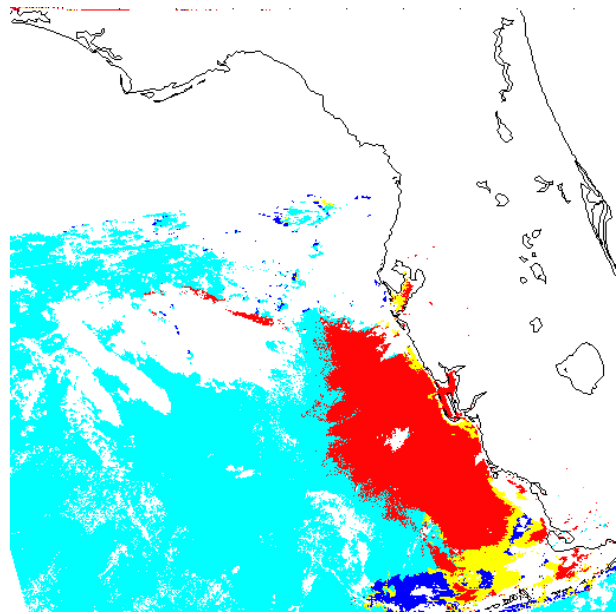
(a) 14 November 1978



(b) 20 November 1978



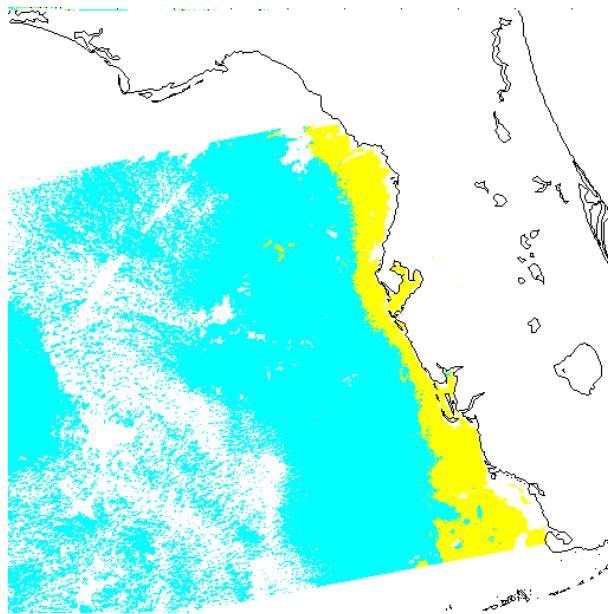
(c) 26 November 1978



(d) 2 December 1978



Figure 9: CZCS images with red tides after processing by the knowledge-guided system. Note (a) is also the training image for the system.



Case I Case II Red Tide "Green River" Unknown

Figure 10: CZCS image without red tides and river plume after processing by the knowledge-guided system.

our approach is significantly more accurate than kNN or a stand-alone neural network. These approaches result in some false positives on images with no red tide or green river in them. To reduce the false positives, a decision threshold at the image level is required. Systems that can do comparable classification on CZCS images do not exist to our knowledge.

Automatic segmentation of CZCS images is a complex task, the system integrates both mrf-FCM, a rule-based system and a NN. The results show that a neural network provides a general approach to extract knowledge from the training images and can be effectively applied to the fuzzy cluster centers to automatically define boundaries for our knowledge-guided system. Under our approach, after training, the system can be used to identify different waters without any human intervention. This is important for satellite image processing, as the periodic collection of the image over a specific geographic area will last several years.

Automatic identification and tracking of particular water types (or phytoplankton blooms) from satellite images would provide an extremely useful tool to address resource management issues and scientific questions regarding the fate of organic material in the seas. Through the use of satellite imagery and automatic segmentation of CZCS images, monitoring capability for coastal blooms can be developed. Timing and sequences of red tides in different geographic areas could be monitored, thereby providing valuable information for marine resource managers. The approach presented in this paper can be used by oceanographers to track and analyze riverine plumes, as well as to estimate their spatial extension.

To improve the accuracy of our knowledge-guided system, more red tides and river plume instances are needed as training/testing sets to calibrate the system. The extent of red tides and river plumes detected using the system needs further verification. On the separation of case I and case II waters, we need to calibrate our system by field measurement. The CZCS-derived pigment concentration suffers a high degree of contamination by colored organic material within coastal and river discharge areas. The suspended sediment concentration in coastal waters also has effects on the intensity observed in satellite imagery. Investigation of these effects on our system needs to be addressed.

The new SeaWiFS[27] sensor on the OrbviewII satellite had come on line late 1997 and it is possible now to visit the areas described here and apply our approach modified for SeaWiFS images[36]. The SeaWiFS provides a radiometric sensitivity superior to CZCS. It also has additional spectral bands, a band near 412nm to separate the detrital and viable phytoplankton signals. The system presented in this paper can be modified to make use of the additional spectral band. After enough SeaWiFS images have been collected and ground-truthed, the system can be trained and used to process new SeaWiFS images.

## 6 Acknowledgments

We thanks Fernando Gilbes, now at the University of Puerto Rico, providing the ground truth CZCS images.

## References

- [1] H. R. Gordon, J. W. Brown, and et. al, “Nimbus-7 CZCS: Reduction of its radiometric sensitivity with time,” *Appl. Opt.*, vol. 22, pp. 3929–3931, 1983.
- [2] H. R. Gordon, D. K. Clark, and et. al, “Phytoplankton pigment concentrations in the middle atlantic bight: Comparision between ship determination and coastal zone color scanner estimates,” *Appl. Opt.*, vol. 22, pp. 20–36, 1983.
- [3] H. R. Gordon and D. K. Clark, “Atmospheric effects in the remote sensing of phytoplankton pigments,” *Boundary-Layer Meteorol.*, vol. 18, pp. 299–313, 1980.
- [4] F. J. Wang, “Fuzzy supervised classification of remote sensing images,” *IEEE Trans. Geoscience and Remote Sensing*, vol. 28(2), pp. 194–201, 1990.
- [5] C. Li, D.B. Goldgof, and L.O. Hall, “Automatic segmentation and tissue labeling of MR brain images,” *IEEE TMI*, vol. 12, no. 4, pp. 740–750, December 1993.
- [6] C. Li, D. B. Goldgof, and L. O. Hall, “Towards automatic classification and tissue labeling of MR brain images,” in *Proc. Int. Workshop on Structural and Syntactic Pattern Recogn.*, 1992.
- [7] R. K. Kiang, “Classification of remotely sensed data using OCR-inspired neural network techniques,” in *IGARSS Symp., Houston, TX, 1992*, vol. 2, pp. 1081–1084.
- [8] G. F. Hepner, T. Logan, N. Ritter, and N. Bryant, “Artificial neural network classification using a minimal training set: Comparison to conventional supervised classification,” *Photogrammetric Engineering & Remote Sensing*, vol. 56(4), pp. 469–473, 1990.
- [9] A. A. Abuelgasim, S. Gopal, J. R. Irons, and A. H. Strahler, “Classification of ASAS multi-angle and multispectral measurements using artificial neural networks,” *Remote Sensing of Environments*, vol. 57, pp. 79–87, 1995.
- [10] M. A. Friedl and C. E. Brodley, “Decision tree classification of land cover from remotely sensed data,” *Remote Sensing of Environments*, vol. 61, pp. 399–409, 1997.
- [11] F. A. Kruse, A. B. Lefkoff, and J. B. Dietz, “Expert system-based mineral mapping in northern death valley, california/nevada, using the airborne visible/ infrared imaging spectrometer(AVIRIS),” *Remote Sensing of Environments*, vol. 44, pp. 309–336, 1993.

- [12] T. A. Warner, D. W. Levandowski, R. Bell, and H. Cetin, “Rule-based geobotanical classification of topographic, aeromagnetic, and remotely sensed vegetation community data,” *Remote Sensing of Environments*, vol. 50, pp. 41–51, 1994.
- [13] L. R. Medsker and D. L. Bailey, “Models and guidelines for integrating expert systems and neural networks.,” in *Hybrid Architectures for Intelligent Systems*, A. Kandel and G. Langholz, Eds., pp. 184–171. CRC Press, 1992, Boca Raton, Florida.
- [14] C. Posey and A. Kandel, “Fuzzy hybrid systems.,” in *Hybrid Architectures for Intelligent Systems*, A. Kandel and G. Langholz, Eds., pp. 174–197. CRC Press, 1992, Boca Raton, Florida.
- [15] M. E. Cohen and D. L. Hudson, “Integration of neural network techniques with approximate reasoning in knowledge-based systems.,” in *Hybrid Architectures for Intelligent Systems*, A. Kandel and G. Langholz, Eds., pp. 72–85. CRC Press, 1992, Boca Raton, Florida.
- [16] M. Zhang, L. O. Hall, and D. B. Goldgof, “Knowledge-based classification of czcs images and monitoring of red tides off the west florida shelf,” *The 13th International Conference on Pattern Recognition (ICPR), Viena, Asutria*, vol. B, pp. 452–456, August, 1996.
- [17] T. W. Cheng, D. B. Goldgof, and L. O. Hall, “Fast fuzzy clustering,” in *FUZZ-IEEE*, 1995, pp. 2289–2295.
- [18] J.C. Bezdek, L.O. Hall, M.C. Clark, and D.B. Goldgof, “Segmenting medical images with fuzzy models: An update,” in *Fuzzy Information Engineering*, D. Dubois, H. Prade, and R. Yager, Eds., pp. 69–92. John Wiley and Sons: New York, 1997.
- [19] K. A. Steidinger and K. Haddad, “Biologic and hydrographic aspects of red tides,” *Bio-Science*, vol. 31(11), pp. 814–819, 1981.
- [20] P. A. Tester and K. A. Steidinger, “Gymnodinium breve red tide bloom: Initiation, transport, and consequences of surface circulation,” *Limnology and Oceanography*, vol. 42(5), pp. 1039–1051, 1997.
- [21] K. L. Carder and R. G. Steward, “A remote-sensing reflectance model of a red-tide dinoflagellate off west florida,” *Limnol. Oceanogr.*, vol. 30, pp. 286–298, 1985.
- [22] F. Gilbes, C. Tomas, , J. J. Walsh, and F. E. Muller-Karger, “An episodic chlorophyll plume on the west florida shelf,” *Continental Shelf Research*, vol. 16(9), pp. 1201–1224, 1996.

- [23] F. E. Muller-Karger, J. J. Walsh, R. H. Evans, and M. B. Meyers, “On the seasonal phytoplankton concentration and sea surface temperature cycles of the gulf of mexico as determined by satellite,” *J. Geophys. Res.*, vol. 96(C7), pp. 12645–12665, 1991.
- [24] A. Morel and L. Prieur, “Analysis of variations in ocean color,” *Limnol. Oceanogr.*, vol. 22, pp. 709, 1977.
- [25] C. W. Brown and J. A. Yoder, “Coccolithophorid blooms in the global ocean,” *J. Geophys. Res.*, vol. 99(C4), pp. 7467–7482, 1994.
- [26] F. E. Muller-Karger, C. R. McClain, R. N. Sambrotto, and G. C. Ray, “A comparison of ship and coastal zone color scanner mapped distribution of phytoplankton in the southern bering sea,” *J. Geophys. Res.*, vol. 95(C7), pp. 11483–11499, 1990.
- [27] SeaWiFS Technical Report Series, *Volume 1, An Overview of SeaWiFS and Ocean Color*, NASA, Goddard Space Flight Center, July, 1992.
- [28] Remote Sensing Group, *DSP User’s Manual*, University of Miami/RSMAS, August 3, 1988.
- [29] C. F. Hutchinson, “Techniques for combining landsat and ancillary data for digital classification improvement,” *Photogrammetric Engineering and Remote Sensing*, vol. 48(1), pp. 123–130, 1982.
- [30] P. J. Werbos, “Backpropagation and neurocontrol: A review and prospectus,” in *International Joint Conference on Neural Networks*, 1989, vol. 1, pp. 209–216.
- [31] J. Giarratano and G. Riley, *Expert Systems: Principles and Programming*, Boston: PWS Publishing, second edition, 1994.
- [32] S. E. Fahlman, “Faster-learning variations on back-propagation: An empirical study,” *Proceedings of the 1988 Connectionist Models Summer School*, pp. 38–51, 1988.
- [33] J. R. Quinlan, *C4.5: Programs for Machine Learning*, Morgan Kaufmann, 1993.
- [34] Simon Haykin, *Neural Networks: A Comprehensive Foundation*, Prentice Hall, 1994.
- [35] G. A. Vargo, K. L. Carder, W. Gregg, E. Shanley, and C. Heil, “The potential contribution of primary production by red tides to the west florida shelf ecosystem,” *Limnol. Oceanogr.*, vol. 32, no. 3, pp. 762–767, 1987.

- [36] W. Yao, "Knowledge-based classification of seaWiFS satellite images for monitoring phytoplankton blooms off west florida," M.S. thesis, University of South Florida, August, 1999.